UNIVERSITA' DEGLI STUDI DI GENOVA

Dottorato di Ricerca in Biotecnologie in Medicina Traslazionale

XXXV cycle

Radiological assessment of muscle mass and quality (sarcopenia) in women with breast cancer

COORDINATORE Prof. P. Malatesta

CANDIDATA Dott.ssa Rossi Federica

TUTOR Prof. Tagliafico Alberto Stefano

Introduction

The term “sarcopenia” etymologically derives from the ancient Greek, composed of the words σάρξ (sárx, “flesh”) + πενία (penía, “poverty, want”). Its first definition was given by Rosenberg et al., who proposed this term to describe the age-related decrease of muscle mass [1]. For many years, sarcopenia has been interpreted as a geriatric syndrome. Indeed, sarcopenia is prevalent in older population, being favored by different factors, such as less-than-optimal diet, bed rest or sedentary lifestyle, chronic disease and certain therapy [2-4]. In terms of human health, sarcopenia is associated with increased risk for hospitalization and increased cost of care [5]. Indeed, it can lead to mobility disorders (resulting in fractures and falls) with loss of independence and it is associated with cardiac and respiratory disease and cognitive impairment [6-7]. However recently, the development of sarcopenia, long associated with ageing and older population, was recognized to begin earlier in life [8]. Indeed, muscle mass vary across a lifetime, with maximal levels reached in young adulthood and decreasing values beyond the age of 50 years. In addition, sarcopenia is influenced by many contributing factors beyond aging [9]. Consequently, in 2018, the European Working Group on Sarcopenia in Older People (EWGSOP) revised the definition of sarcopenia [10]. Specifically, sarcopenia was defined as a loss of muscle strength, confirmed by the presence of low muscle quantity and quality [10]. Sarcopenia can be divided in “primary” (or age-related), when no other specific cause

is recognized, and in “secondary”, when causal factors other than ageing are evident [10]. Secondary sarcopenia can be a consequence of a systemic disease, especially one that induces an inflammatory response through systemic cytokine-mediated cascade [11]. This inflammatory activity leads to a pro-catabolic state (with mobilization and degradation of protein), wherein protein degradation outweighs protein synthesis, and consequentially to a loss of skeletal muscle mass [11]. Skeletal muscle mass can be considered a key regulator of metabolic and inflammatory pathways, so the development of sarcopenia promotes a generalized inflammatory state [11]. In addition, sarcopenia has been widely recognized as a predictor for mortality and the development of chronic diseases [12,13]. These assumptions have been widely demonstrated by large longitudinal studies using low muscle mass or low grip strength as potential biomarkers [12,13]. Using Medical imaging it has been shown that a loss up to 40% of the muscle cross sectional area could occur between the age of 20 to 60 depending on anatomical site, muscle examined and even gender. For example, Janssen *et al.* reported a loss of 1.9 and 1.1 kg absolute muscle mass per decade in men and women, respectively [14]. Muscle mass and muscle quality are both important. Indeed, recent literature shows that the muscle composition, the ratio between fat and muscular tissue, contributes largely to the observed muscular weakness, predominantly caused by a reduction of type II fibers [15].

Cancer is probably one of the major causes of secondary sarcopenia, being a condition associated with age and comorbidities, malnutrition and physical inactivity [16,17]. A recent meta-analysis showed that there is an association between

sarcopenia and prognoses in various types of cancers. N=7843 patients from 38 studies were included in the meta-analysis and skeletal muscle index (SMI) lower than cut-offs was associated with poor overall survival (OS) (HR = 1.44, 95% CI = 1.32-1.56, $p < 0.001$) [17]. In addition, cancer therapy could affect skeletal muscle change, for example some chemotherapy drugs (e.g., cisplatin, irinotecan and doxorubicin) cause direct muscle loss through activation of the transcription factor NF kappa B, with up-regulates ubiquitin and proteasomes, increases proteolysis and inflammatory cytokines (IL-1beta, IL6 and TNF alpha) which increases E3 ligases (atrogin-1) and increases ubiquitin protein binding for proteolysis [16]. TNF alpha accelerates catabolism (protein loss, insulin resistance), muscle contractile dysfunction, and disrupts myogenesis leading to muscle weakness [16]. In addition, chemotherapy can induce oxidative stress and can increase reactive oxygen species (ROS) in muscle. Chemotherapy can lead to mitochondrial damage, with cytochrome C reduction and peroxisome proliferation [16]. Sarcopenia is considered a negative prognostic factor for disease progression and survival, in many types of cancer, including breast cancer (BC). Prado et al. observed that sarcopenia was associated with a higher incidence of chemotoxicity and a shorter time to tumor progression in metastatic breast cancer patients treated with capecitabine [18]. Villaseñor et al. reported that breast cancer women with sarcopenia had an increased risk of overall mortality [19].

Studies results highlight the potential use of body composition assessment to improve patient's outcome. Therefore, many methods were used to measure muscle quantity

and quality. Dual-energy X-ray absorptiometry (DXA) is a widely available and non-invasive method to assess muscle quantity, with a relatively low radiation exposure (0.001 mSv approximately, less than a standard chest radiography). However, even if correctly performed, DXA could over-/underestimate sarcopenia due to the low accuracy in estimating truncal fat and muscle and to the inability to distinguish obesity from the amount of fat and muscle interpolated from arms and legs [20]. Computed Tomography (CT) is considered the gold standard technique to assess body composition, especially in cancer patients. Indeed, CT is routinely performed in the diagnostic pathway of cancer patients [18,20]. One of the simplest methods to assess skeletal muscle mass in CT, is to measure the psoas muscle area on axial image at the level of the third (L3) or fourth (L4) lumbar vertebra. At the level of L3, rectus abdominis, transverse abdominis, internal and external obliques, quadratus lumborum, psoas major and minor and erector spinae can be evaluated [20; **Figure 1**].

Figure 1. Normal (left image) versus sarcopenic cancer patients (right image) [17].

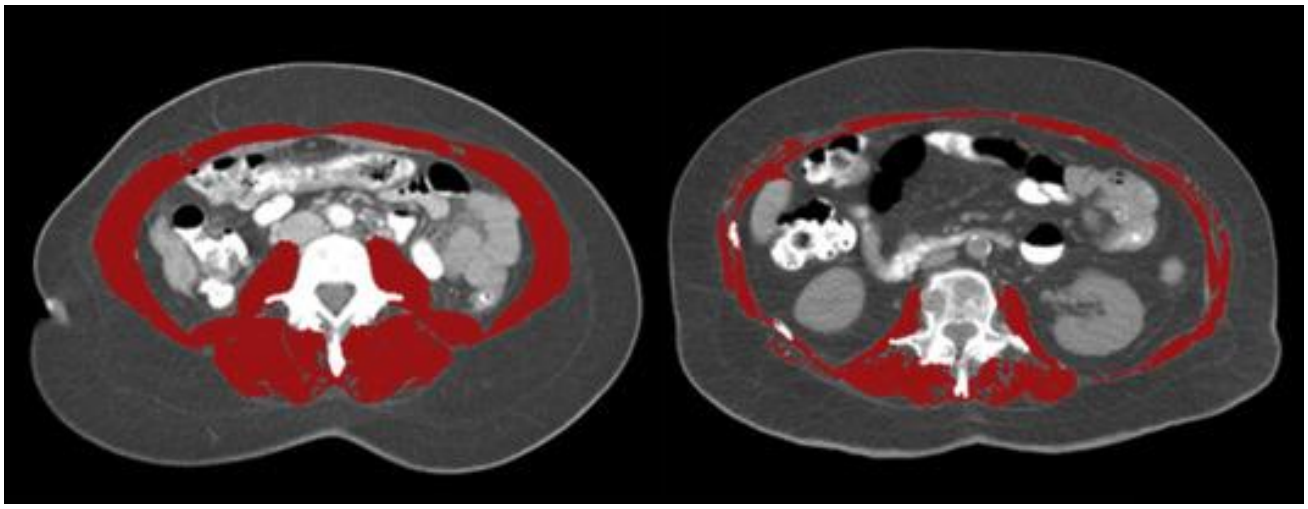

CT also allows to determine muscle density (using a threshold range of 29 to 150 Hounsfield Unit to define muscle tissue) [20]. Even if there is no consensus on standardized CT thresholds to diagnose sarcopenia, generally a Skeletal Muscle Index (SMI) < 41 cm^2/m^2 or < 38.5 cm^2/m^2 is considered the cutoff to define sarcopenia [20]. However, the most important CT disadvantage, is the use of radiations (8 mSv radiation dose typical of an abdomen/pelvis CT). Therefore, CT cannot be proposed as a screening method for sarcopenia [20]. Recently, some studies demonstrated that skeletal muscle mass and sarcopenia can interchangeably be assessed on CT and Magnetic Resonance Imaging (MRI) scans. MRI, mainly used in research settings, guarantee a high contrast resolution and accuracy to assess muscle composition due to the different numbers of protons inside muscular and fatty tissue [20]. Therefore, MRI can detect intra-muscular edema, fibrous involution and even muscular elasticity

and contraction [20]. In addition, MRI is a safety radiation-free imaging technique, but very expensive and not easily available.

Zwart et al. confirmed that neck musculature at the level of third cervical vertebra (C3), used to diagnose sarcopenia in head and neck cancer patients, can be determined with neck MRI scans, even when CT scan is not performed [21]. Rossi et al. demonstrated a strong correlation between psoas muscle area assessed on axial body CT images at the level of the L3 vertebra and pectoralis muscle area (PMA) assessed on MRI in breast cancer (BC) patients [22].

BC is the most frequently diagnosed cancer in women worldwide with 2.26 million new cases in 2020 and represents the leading cause of cancer death in women worldwide [23]. In Italy, approximately 55.000 new diagnosed cases per year and 13.000 deaths are estimated, with a 5-years survival of 87%. [24]. Even if the number of incident cases of breast cancer in Italy is constantly increasing (+0.3% per year), there is a decrease in mortality (-0.3% per year) [24]. The slight increase in incidence could be partly explained by the use of national mammography screening programs. However, significant regional differences still exist today, as demonstrated by a higher incidence in northern Italy (161.9 cases/100.000 women) than in central (141.7 cases/100.000 women) and southern Italy (124.9 cases/100.000 women) [24]. The reduction in mortality can also be explained by the increased adherence to screening programs, with early diagnoses and better therapeutic strategies [24]. Mammography (MX), the mainstay in BC screening and diagnosis, is a two-dimensional imaging technique, able to identify morphologic findings that are

suspicious for BC, such as masses, microcalcification and architectural distortion, that need further investigation [25]. Ultrasound (US) is frequently used as a supplementary tool to characterize a mammographic abnormality, to determine whether a mass is solid or cystic and to discriminate benign from malignant findings [25]. Breast MRI play an important role for diagnosing BC, together with MX, US and image-guided needle biopsy. According to EUSOBI guidelines, MRI, due to its high sensivity, is an excellent screening modality in high-risk women, with a familial increased risk for BC or who are carriers of gene mutations (e.g., BRCA1 and BRCA2) [26]. MRI is also widely used in preoperative staging (to assess disease extent, look for satellite lesion, exclude contralateral BC) and is considered the best imaging technique to evaluate breast implants [26]. EUSOBI group recommended the use of MRI in occult primary BC in women with metastasis and negative MX and US [26]. MRI is also considered the best imaging modality to assess neoadjuvant chemotherapy (NAC) response [26]. In general, disease stage should be assessed according to the TNM system. In early breast cancer in which asymptomatic distant metastases are very rare, routine staging evaluations are directed al locoregional disease with MX, US and MRI. CT exam must be considered for women with advanced disease, with clinically positive axillary lymph nodes, large tumors, aggressive biology or clinical signs, symptoms or laboratory values suggesting distant metastases [24]. Therefore, CT exam is not systematically used to assess extension in BC patients. Even if CT remains the gold standard method to measure sarcopenia, MRI can represent a valid alternative to evaluate the loss of muscle mass when CT

examination is not available. In addition, recent studies have shown that MRI evaluation of the pectoralis muscle mass is an easily reproducible method between radiologists, as demonstrated by good inter- and intra-reader agreement and it requires neither time nor additional protocols [27].

Therefore, the aim of my PhD was to study with radiological techniques the muscle mass variation in women with breast cancer recruited both prospectively and retrospectively at IRCCS Ospedale Policlinico San Martino, a 1200-bed teaching hospital in Genoa, Northern Italy. In particular, I tried to develop and test a new method to assess muscle mass on breast MRI for breast cancer patients, especially when body CT is not available.

Chapters

1. Breast MRI: pectoralis muscle assessment.

According to EUSOBI guidelines, breast MRI, MX, US and Tomosynthesis are recommended in women with early BC for routine staging evaluation of locoregional disease and for treatment follow-up [26]. As said before, CT is recommended in women with advanced disease, with clinically positive axillary lymph nodes, large tumors, aggressive biology or clinical signs, symptoms or laboratory values suggesting distant metastases [24]. Therefore, CT exam is not systematically used to assess extension in BC patients. Even if CT remains the gold standard method to measure sarcopenia, MRI can represent a valid alternative to evaluate the loss of muscle mass when CT examination is not available. Therefore, the first aim of my research was to find if there was a correlation between psoas muscle area assessed on CT images and pectoralis muscle area assessed on breast MRI. Therefore, we decided to review the images of all consecutive BC patients who underwent both total-body CT and breast MRI in our university hospital between January 2016 and January 2018. The period between the two examinations not longer than 4 months, considered as an adeguate follow-up time. We excluded patients with breast sub-muscular implants or with sub-glandular prosthesis. A total of 26 women (mean age 51.1 ± 12.6 years, range 30–76 years) were included in the study. For each woman, we collected clinical data and information on the primary tumour.

Image analysis: CT

All CT scans were acquired with different GE (GE Healthcare) CT scanners. All CT scans were performed with the patient in the supine position, head first on the scanner table and with the arms raised and placed behind the patient's head, out of the scan plane. The whole body was scanned from the lung apex to the pubic symphysis. We analyzed reconstructed axial images with both a 1.25-mm and a 5-mm slice thickness using the software installed on the workstations of our radiology department (Suite-Estensa 1.9-Ebit-Esaote Group Company. 2015). The third lumbar vertebra (L3) was used as a bony landmark to properly identify the psoas muscle. We identified L3 couting down vertebrae from the cervical spine using multiplanar reformatted (MPR) images. Subsequently, we manually contoured the psoas muscle bilaterally and calculated the muscle mass cross-sectional area (square millimetres) (**Figure 2**).

Figure 2. An example of measurement of psoas muscle area (blue area) on axial CT image.

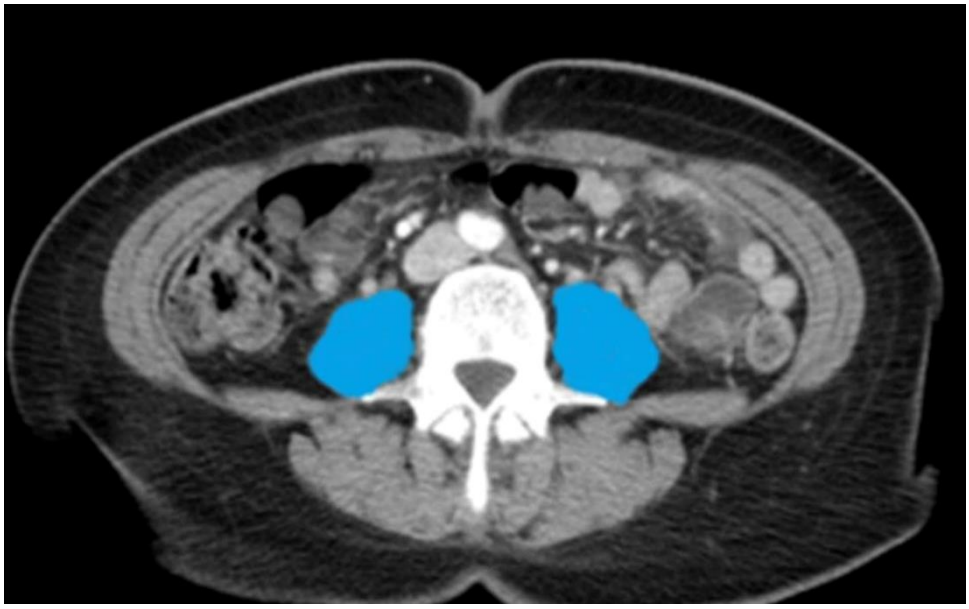

Image analysis on reconstructed axial images with 1.25-mm and 5-mm slice thickness was performed independently by two board-certified radiologists (A.T., with more than 10 years of experience specialised in oncological imaging and in breast imaging and E.B. with more than 5 years of experience in oncological imaging) to assess inter-reader variability. To assess intra-reader agreement, 4 weeks after the first evaluation, all measurements were calculated again by the same two radiologists.

Images analysis: MRI

All patients were examined by using a 1.5-Tesla equipment (Magnetom Avanto, Siemens Healthcare) with dedicated double breast coil. According to international

guidelines, for each patient, we used a standard MRI protocol: axial T2-weighted fast spin echo and axial T1-weighted 2D spoiled gradient echo dynamic contrast-enhanced acquisition with fat saturation, first performed before contrast administration and repeated multiple times after contrast administration. We performed image analysis using the software installed on the workstations of our radiology department as done for CT images. We identified the pectoralis muscle at the level of the sternal angle of Louis (manubriosternal joint that lies at the level of the second costal cartilage) used as bony landmark. Two radiologists (A.T., more than 10 years of experience in oncological imaging and in breast imaging and F.R., 5 years of experience in musculoskeletal imaging) manually contoured the pectoralis muscle area bilaterally and measured the cross-sectional area (square millimetres) on axial pre-contrast T1-weighted gradient echo fat-saturated images. Intra- and inter-observer agreement for PMA was evaluated as well.

Statistical analysis

We performed descriptive statistical analysis using statistical software [SPSS, version 12.0.1 (SPSS, Inc.); Excel 2007 (Microsoft Corp.]. The aim was to calculate inter- and intra-reader agreement in assessing the psoas cross-sectional area (square millimetres) on CT axial images with 1.25-mm and 5-mm slice thickness and then the PMA in square millimetres on MRI axial pre-contrast T1-weighted gradient echo fat-saturated images. Cohen's kappa test was used to evaluate inter-reader agreement. A p value of 0.05 was considered statistically significant. To evaluate the correlation between the PMA on MRI and the psoas muscle area on CT, the two-tailed Pearson's

test was performed using both 1.25-mm slice thickness and 5-mm slice thickness. The Pearson *r* correlation coefficient with 95% confidence intervals (CI) and the coefficient of determination (R^2) were calculated. A *p* value of 0.05 was considered statistically significant. To have a significant correlation of an $r = 0.06$ with a type I error of 0.05 a total sample size of 19 was calculated as sufficient.

Results

According to inclusion criteria, 2/28 (7.1%) women were excluded for missing data. Therefore, a total of 26 BC patients were included in the study (mean age 51.1 ± 12.6 years, range 30–76 years; mean cancer size ± standard deviation 21 ± 11 mm). Clinical data and cancer features (size and type, histological grade, lymph node status, oestrogen and progesterone receptors, human epidermal growth factor receptor 2) were retrievable for 24/26 (92.31%). Mean values and standard deviation for measurement data were also reported (**Table 1**).

Table 1: clinical data and cancer features

Clinical data and cancer characteristics		Number and percentage
ER status	Positive	16/24 (66.67%)
	Negative	8/24 (33.33%)
PR status	Positive	16/24 (66.67%)
	Negative	8/24 (33.33%)
HER2/neu status	Positive	10/24 (41.67%)
	Negative	14/24 (58.33%)
Histological grade	I	0
	II	11/24 (45.83%)
	III	13/24 (54.17%)
Cancer type	IDC	20/24 (83.33%)
	ILC	4/24 (16.67%)
Lymph node status	Positive	9/24 (37.50%)
	Negative	15/24 (62.50%)
Total psoas area (1.25-mm slice thickness CT)	Mean value	466.02 mm^2
	Standard deviation	206.38 mm^2
Total psoas area (5-mm slice thickness CT)	Mean value	509.96 mm^2
	Standard deviation	226.82 mm^2
Pectoralis muscle area (axial T1-weighted fat saturated images)	Mean value	793.30 mm^2
	Standard deviation	455.84 mm^2

Cancer type, histological grade, lymph node status, oestrogen and progesterone receptors, human epidermal growth factor receptor 2 were retrievable for 24/26 (92%). Mean values and standard deviation for measurement data were also reported
ER oestrogen receptor, *PR* progesterone receptor, *HER2* human epidermal growth factor receptor 2, *IDC* invasive ductal carcinoma, *ILC* invasive lobular carcinoma, *CT* computer tomography

Inter- and intra-reader agreement

On axial 1.25-mm-slice-thickness CT images, according to Cohen's kappa test, the inter-reader agreement was considered almost perfect (0.81–1). The inter-reader agreement was $k = 0.85$, $p < 0.05$. On axial 5-mm-slice-thickness CT images inter-reader agreement was considered good (0.61–0.8). The inter-reader agreement was $k = 0.79$, $p < 0.05$. Intra-reader agreement of reader 1 was 0.98 and 0.94 for 1.25-mm and 5-mm, respectively. Intra-reader agreement of reader 2 was 0.95 and 0.94 for 1.25-mm and 5-mm, respectively.

On axial pre-contrast T1-weighted gradient echo fat-saturated MR images, the inter-reader agreement was 0.61, $p < 0.05$, considered good (0.61–0.8).

Intra-observer agreement of reader 1 and reader 2 for PMA estimation were good (0.62 and 0.64).

Correlations

Comparing axial 5-mm-slice-thickness body CT images and T1-weighted fat-saturated MR images, the Pearson r correlation coefficient was 0.52 (95% CI0.20 – 0.78). Comparing axial 1.25-mm slice thickness body CT images and T1-weighted MR images, the Pearson r (– 1 < r < + 1) correlation coefficient was 0.70 (95% CI 0.41–0.81) and the coefficient of determination was 0.49, $p < 0.05$ (**Figure 3**).

Figure 3. Correlation between total psoas area (TPA) and pectoralis muscle area (PMA)

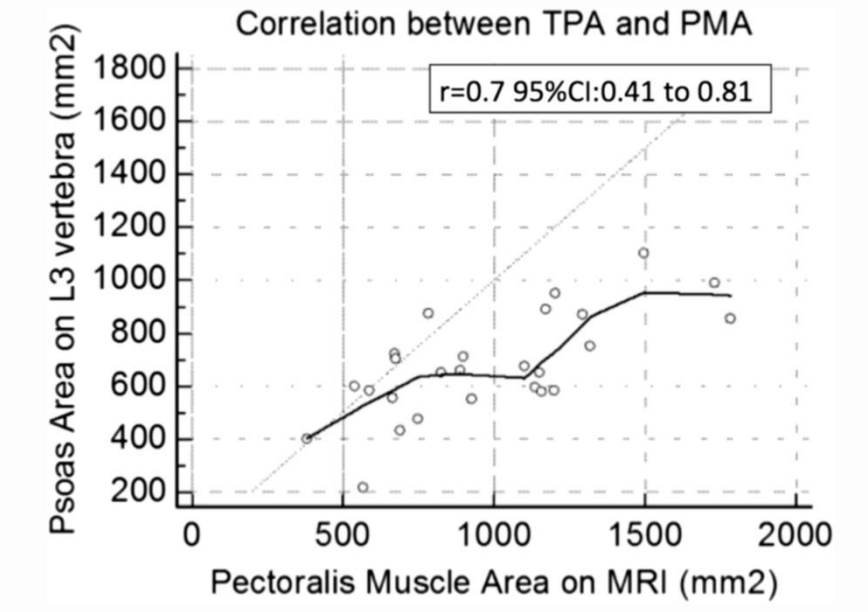

Discussion

The results of our first study demonstrated a strong correlation between the PMA assessed on breast MRI and the psoas muscle area assessed on body CT images. In addition, the technique for measurement of PMA has also been shown to be highly reproducible between different readers.

2. **Pectoralis muscle assessment: Model development**

Pectoralis muscle assessment and MRI

PMA evaluation represented a new method that could be used to evaluate BC patients' muscular status directly on breast MRI even without body CT. Our initial results provided some evidence of potential clinical utility of PMA assessment. PMA measurement technique resulted to be easily reproducible.

We decided to develop and patent our own method for evaluating PMA. Continuing our research in this field, we have noticed that the precise

Lewis angle identification could be difficult and often not optimal due to womens' anatomy and image artifacts. Therefore, we decided to measure the pectoralis muscle area at about 1-1,5cm from the angle of Louis. The measurement can be easily obtained by knowing the slice thickness on axial sequences, for example if the slice thickness on axial plane is 4mm, we calculate about 3 slices (4x3mm=1,2cm) from the angle of Louis. The method provided the analysis on axial FLASH T1-weighted

images before contrast media administration to obtain the best spatial and contrast resolution (**Figure 4**). Images before contrast administration were used to make our method available even in abbreviated MRI screening protocols (without contrast media administration) even in non-high-risk populations. On CT scan, we can speak about sarcopenia when the skeletal muscle index (SMI) is below 41cm^2/m^2, value that is obtained dividing muscle area at L3 in cm^2 by patient height in meters squared (m^2). Considering that the pectoralis muscle area correlates proportionally with the psoas muscle area, using a proportion, we obtained a cut-off dividing muscle area by patient height, value that is commonly obtain before each MRI examination.

Formula: psoas muscle area: pectoralis muscle area= cut-off SMI of the psoas: cut-off SMI of the pectoralis

According to literature data, the cut-off of the pectoralis muscle mass on breast MRI is about 5,6cm^2/m^2 ±2 (standard deviation). The method could be easily applied in all BC stages.

Pectoralis muscle mass and Breast Ultrasound and ABVS (Automated Breast Volume Scanner)

To test our method, we also tried to apply it to other imaging technique. EUSOBI recommended the use of breast US for suspected cancer at all ages, also in young women (under 40 years) [26]. When there is a suspicious finding US-visible, US-guided biopsy is suggested, even for palpable lesions [26]. During breast US examination, the pectoralis muscle can be evaluated using linear high-frequency probe (7-15 MHz). Indeed, the pectoralis muscle is superficial and can be easily recognized with optimal spatial resolution. The angle of Louis can be manually recognized and used as a bony landmark, from about 1-1,5 cm caudally, the anteroposterior thickness of the pectoralis, both on axial and transverse scans, can be measured. Finally the PMA can be calculated from the thickness using the ellipsoid formula. The PMA obtained is divided by patient's height to calculate the skeletal muscle index (SMI). The method can have a potential use assessing muscle mass in BC patients, in particular in young women and in patients with breast implants above the pectoralis muscle. Our method can also be applied during the use of the ABVS, Automated Breast Volume Scanner, a new imaging technology using high-frequency waves (18MHz), alternative to tradition hand-held US. It is an operator-independent standardized method that provides physicians with a 3D volumetric image of the entire breast. With the ABVS, a 3D volumetric imaging and unique coronal view can be obtained. Consequentially, PMA can be easily evaluated as previously shown for the 2D US.

Our new method has been published and patented. It could be applied for muscle mass composition assessment in BC women, also in early stage patients, that, according to international guidelines, normally underwent breast MRI and US [26]. One of the biggest benefits is the reproducibility of the method itself, without additional costs or additional examination. According to literature, a careful evaluation of the body composition in BC women could represent an important way to prevent chemotherapy toxicity and to improve quality of life, treatment response and survival [18,19].

Figure 4. An example of pectoralis muscle (orange area) assessment on breast MRI.

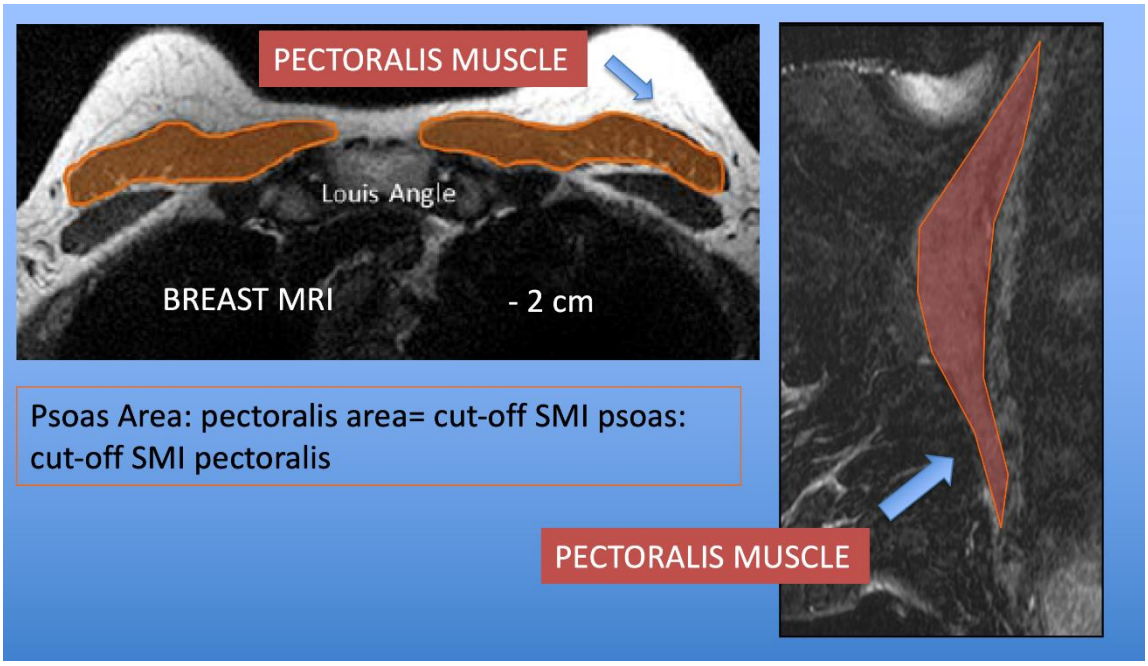

3. Breast MRI: clinical assesment in BC patients underwent neoadjuvant chemotherapy (NAC).

The third step of our research focused on the clinical applicability of our method, in particular we wanted to evaluate whether the PMA, assessed on breast MRI, varied in BC women, who underwent NAC. Neoadjuvant Chemotherapy (NAC) indicates a type of systemic therapy administered prior to surgery, initially used in inoperable BC to make them resectable [28]. Subsequently, it has also been proposed in operable BC, due to fact that NAC could reduce the extent of surgery (breast-conserving surgery and axillary lymph node dissection) [28]. In addition, NAC can eradicate micro-metastatic disease, preventing distant recurrence [28]. After starting NAC, BC women need to be periodically monitored for response with both clinical examination and MRI. International guidelines suggest the use of MRI, considered the best imaging modality to follow BC in the neoadjuvant setting [26].

Materials and Methods

Patient selection and study design

Therefore, we conducted a retrospective study approved by our institutional review board (CER009/2018) and conducted in accordance with the Declaration of Helsinki. A total of n= 110 women treated with different protocol of NAC for histologically and surgically proven primary breast cancer between January 2017 and January 2019 and in whom tumor response was checked with MRI were included. Each patient underwent at least two MRI exams, before starting NAC and after completing NAC.

Based on the recommendations from the EUSOMA working group, post-NAC breast MRI was performed 2 weeks after the last NAC cycle and within 2 weeks before surgery without treatment delay [29]. We excluded women with stage IV BC, or with tumor that demonstrated direct extension to chest wall or skin or with tumor that invaded the pectoralis muscle mass. When MRI examinations before and-or after NAC were not retrievable or of poor diagnostic quality due to artifacts, patients were excluded. We also excluded women with previous breast surgery or with a history of previous systemic treatment. According to these exclusion and inclusion criteria, a total of n=101 BC patients (mean age 56 ± 11 years, range 33–84 years) were finally included. For each woman we collected clinical and histopathological data (pretreatment estrogen and progesterone receptor status, human epidermal growth factor receptor status (HER-2), Ki-67 expression, lymph node status, histological type, average lesion size, molecular categories, and grade). The NAC regimes consisted of epirubicin + 5-fluorouracil + cyclophosphamide (FEC), pertuzumab + paclitaxel + trastuzumab, and epirubicin + cyclophosphamide (EC) followed by paclitaxel. Patients with human epidermal growth factor receptor 2 (HER-2)–expressing tumors were administered trastuzumab for 1 year. The number of cycles of NAC varied from 4 to 6 according to the type of protocol applied. In order to evaluate the response to NAC, we followed the Response Evaluation Criteria in Solid Tumors (RECIST) on MRI, as previously done [30,31].

MRI examination and image analysis

Breast MRI was performed on a 1.5-T equipment (Magnetom Avanto, Siemens Healthcare) using a dedicated double breast coil in prone position. We used a standard MRI protocol as done before, based on the use of axial turbo inversion recovery magnitude (TIRM) sequence and axial 3D fast low-angle shot (FLASH) T1-weighted images, first performed before contrast administration and repeated multiple times after contrast administration (0.1 mmol of GD-DTPA/kg of body weight at a rate of 2 mL/s, followed by a 20 mL saline flush). Image analysis was performed independently by two radiologists with more than 5 and 2 years of experience in both musculoskeletal and breast radiology. According to our published method, the pectoralis muscle area was manually contoured on axial 3D FLASH precontrast T1-weighted images. Cross-sectional area (square centimeters) of the average value for bilateral pectoralis muscles was calculated for each woman.

Statistical analysis

Statistical analysis was conducted using the non-parametric Wilcoxon-Mann-Whitney U test, in order to compare the median values and percentage changes of PMA on MRI examinations, acquired at the beginning of NAC and at the end of NAC. We also performed a multivariate regression analysis on ΔPMA (PMApre-PMApost) to evaluate if muscle mass loss correlated with age, time between MRI exams, estrogen and progesterone receptor status, human epidermal growth factor receptor status (HER-2), Ki-67 expression, lymph node status, RECIST criteria,

histological type, molecular categories, and grade. A $p < 0.05$ were considered statistically significant. Inter- and intra-reader agreement were also calculated using Cohen's kappa test.

Results

According to the study design, a total of 9/110 (8%) BC patients were excluded for missing or incomplete data. Indeed, in 5/9 patients (55.6%) pre-NAC MRI examinations were not retrievable and 4/9 patients (44.4%) were excluded because of previous breast surgery and radiotherapy. A total of $n = 101$ BC patients were finally included in the study. Standard clinical characteristics were retrievable for all included patients (**Table 2**).

Table 2. Clinical characteristics of n = 101 BC patients

	Complete response (*n* = 36)	**Partial response (*n* = 49)**	**Stable disease (*n* = 12)**	**Progressive disease (*n* = 4)**
	Number of cases	**Number of cases**	**Number of cases**	**Number of cases**
Age (years)				
≤ 50	18	12	2	1
> 50	16	37	12	3
Grade				
1	2	1		
2	20	28	5	3
3	14	20	7	1
Estrogen receptor				
Positive	20	34	5	0
Negative	16	15	7	4
Progesterone receptor				
Positive	17	22	4	0
Negative	19	27	8	4
HER-2+				
Positive	10	8	3	0
Negative	26	41	9	4
Ki67				
Positive	25	28	9	4
Negative	11	21	3	0
Lymph node invasion				
Positive	8	14	4	1

Negative	28	35	8	3
Molecular categories				
Luminal A	16	28	8	0
Luminal B	7	5	2	0
Triple negative	8	12	2	4
HER-2+	5	4	0	0
Histological type				
Invasive lobular carcinoma	3	2	2	1
Invasive ductal carcinoma	32	45	10	3
Mucinous carcinoma	0	2	0	0
Carcinosarcoma	1	0	0	0
Average lesion size (cm)				
< 5	10	14	7	3
> 5	26	35	5	1
Stages				
IIA	14	11	2	0
IIB	12	18	3	3
IIIA	10	20	7	1

The average lesion size was 35.1 ± 16 mm. Time between the two MRI examinations, before starting NAC and after NAC, was 166.8 ± 50 days (**Table 3**).

Table 3. Different regimes of neoadjuvant chemotherapy (NAC)

Drug	**Number of patients**	**RECIST**			
		Complete response (*n* = 36)	**Partial response (*n* = 49)**	**Stable disease (*n* = 12)**	**Progressive disease (*n* = 4)**
		Number of cases	**Number of cases**	**Number of cases**	**Number of cases**
Epirubicin + 5-fluorouracil + cyclophosphamide (FEC)	11	1	4	4	2
Pertuzumab + paclitaxel + trastuzumab	9	5	4	0	0
Epirubicin + cyclophosphamide (EC) followed by paclitaxel	81	30	41	8	2

PMA calculated pre-NAC (mean value 8.114 cm^2) resulted to be larger than PMA calculated post-NAC (mean value 7.032 cm^2, $p < 0.001$, delta value 0.963) (**Figure 5**).

Figure 5. Pectoralis muscle mass variation before and after NAC. Pectoralis muscle area calculated pre-NAC (green line) is larger than pectoralis muscle area calculated post-NAC (blue line).

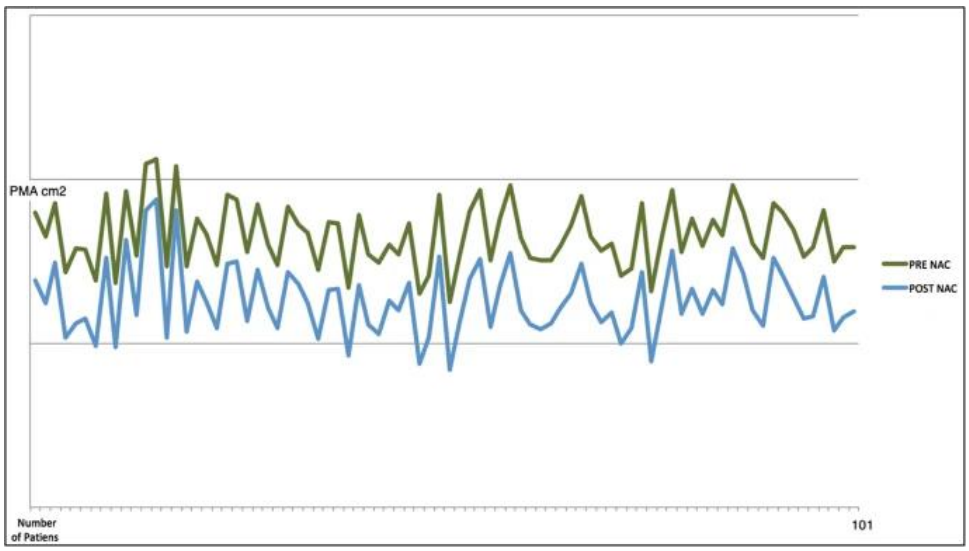

According to the RECIST criteria, no significant differences between responders (complete or partial response) and non-responders were found (p = 0.362).

The multivariate regression analysis did not demonstrate any significant relationships between ΔPMA and clinical and histopathological data. Among the possible explanations of this result, the hypothesis that the PMA could be considered an independent indicator for the muscle mass evaluation in BC women undergoing NAC should not be excluded.

Cohen's kappa test demonstrated good inter-reader and intra-reader agreement (*k* value between 0.61 and 0.8). The inter-reader agreement was $k = 0.72$, $p < 0.05$, and the intra-reader agreement of radiologist 1 and radiologist 2 were respectively 0.69 and 0.71.

Discussion

The results of this part of my research provide some evidence of potential clinical utility of PMA assessment in BC women. Indeed, the study demonstrated that

PMA declined during NAC suggesting that the loss of skeletal muscle mass could be monitored during breast MRI examinations. To explain the loss of PMA during NAC, a multifactorial cause, partly due to pharmacokinetics and to inflammatory cell recruitment was supposed. In addition, one of the most frequently reported adverse events during NAC is asthenia, related to the muscle loss. Pectoralis muscle mass variation assessed on breast MRI may help the evaluation of the risk of toxicities and may optimize patient selection for specific therapeutic protocols with better clinical outcomes.

4. Breast MRI in young women under 45 with BC

The final part of my research focused on the applicability of the method to young women of reproductive age (≤45 years) with BC. Indeed, our hospital is a reference center. although the likelihood of developing BC is higher in women ≥ 50 years, BC is the most common tumor type in young women of reproductive age [32]. About 7% of breast cancer cases are diagnosed in women ≤45 years, that is more than 40% of all cancers affecting this age group [32]. BC in young women seems to be more aggressive, with reduced survival [33]. Indeed, BC in young women is characterized by unfavorable biology, with higher proportion of grade 3, triple-negative and human

epidermal growth factor receptor 2 (HER-2) overexpression, lymph vascular invasion, lymphocytic infiltration and higher proportion of basal-like tumors [33]. Regarding risk factors, hormonal factors (including early menarche, oral contraceptives, anovulatory infertility and late parity after age 30) increase BC risk even among young women [33]. In addition, in females of younger age breast density, recognized as an independent BC risk factor, is higher and represents an indication for pre-operative MRI [33]. However, it is important to underline that in young women, BC is frequently familial, and approximately half of these patients harbor a gene mutation in BRCA1, BRCA2 or TP3 and about 13-19% of young women reported a first-degree relative affected by BC [33]. As said previously, MRI is widely recommended as screening modality in these high-risk women [26,29]. In addition, MRI plays a pivotal role in the early detection and staging of BC in young women. Invasive ductal carcinoma (IDC) is the most common BC type for women of all ages; however, a higher proportion of young women are diagnosed with this type compared with older patients (87% vs 78%). Women of reproductive age with IDC seem to have a significantly lower 5-years relative survival rate than patients age over 40 (83% compared with 88%). Invasive lobular carcinoma (ILC) represents the second most common BC type in young women. In patients with ILC, a preoperative MRI is strongly recommended because it is often multifocal or multicentric and complicated by concurrent contralateral carcinomas [26]. In addition, the biological aggressiveness (e.g., high-risk HER2-positive or triple-negative breast cancer) of BC in young women requires the use of NAC regimens, whose response is evaluated

with MRI [26]. Indeed, women who have undergone NAC should be monitored for response with periodic breast imaging surveillance [28]. Therefore, MRI has different indications and could represent a valid tool to evaluate sarcopenia in young women, without additional protocols and diagnostic delays, even when CT is not available. Indeed, early diagnosis and treatment of skeletal muscle loss could improve young patients' outcome, diminishing morbidity and mortality. The purpose of this final part of the research was to evaluate if the PMA, assessed on consecutive MRI examinations, varies, reflecting the loss of skeletal muscle mass, in young women with invasive ductal breast cancer undergoing NAC. In addition, the study aims to evaluate if there is a correlation between sarcopenia and NAC, biological features and radiological response to treatment.

Materials and Methods

Patient selection and study design

The study was approved by our institutional review board (CER009/2018) and carried out according to the criteria set by the Declaration of Helsinki. We included a total of 65 consecutive young patients of reproductive age (≤45 years) that were enrolled in the coordinating center of the PREgnancy and Fertility (PREFER) study (NCT02895165), a prospective research investigating BC patients' preferences and choices towards the available strategies for ovarian function and fertility preservation [34]. The included patients have undergone different regimes of NAC for histologically proven primary IDC, whose clinical and radiological response was

evaluated in our University Hospital from January 2019 to September 2021. Each patient underwent consecutive MRI examinations, used to assess radiological response to NAC. Therefore, MRI examinations were performed before the initiation of NAC therapy and repeated after the completion of NAC before surgery. To avoid delays in surgical treatment, post-NAC MRI was conducted 2 weeks after the last therapeutic cycle and within 2 weeks before surgery, as recommended by the EUSOMA working group [29]. In addition, MRI was performed in the second week of menstrual cycle (day 6–13 counting from the first day of bleeding) [26]. MRI images were retrospectively analyzed for each young woman.

Inclusion criteria were as follows:

1) Young women of reproductive age (≤45 years) enrolled in the PREFER study, who received a diagnosis of IDC, histologically confirmed by core needle biopsy.
2) Each patient selected must have undergone MRI examinations before and after NAC in our Institution with standard protocol.
3) For each patient, pretreatment progesterone (PR) and estrogen (ER) receptor status, human epidermal growth factor receptor 2 (HER-2) status, Ki-67 expression and lymph node status were collected, based on pretreatment core biopsy.

We excluded patients with:

1) tumor that invades the pectoralis muscle area were excluded to avoid errors in the evaluation of muscle mass.
2) Unknown or incomplete immunohistochemical markers
3) MRI examination both before and after NAC not available
4) MRI images poorly diagnostic because of artifacts, such as susceptibility artifacts due to infusion port
5) Previous history of breast surgery, for example with breast implants
6) history of previous systemic, surgical or radiotherapy treatment that may have influenced body composition

Neoadjuvant Chemotherapy

According to international guidelines, the young patients of reproductive age with IDC, included in this study, have undergone one of following NAC therapies:

- 4 cycles of EC (Epirubicin and Cyclophosphamide) and weekly Paclitaxel for 8-12 weeks
- 4 cycles of EC (Epirubicin and Cyclophosphamide) followed by 8-12 weeks of Carboplatin and Paclitaxel
- 4 cycles of EC (Epirubicin and Cyclophosphamide) followed by 8-12 weeks of Paclitaxel and Herceptin (Trastuzumab)
- 8-12 weeks of Paclitaxel and Carboplatin

After starting NAC, BC young patients were periodically monitored for response with both clinical examination and MRI, considered the best imaging modality to follow BC in the neoadjuvant setting. To assess radiological and clinical responses to therapies, the "Response Evaluation Criteria in Solid Tumors (RECIST)" were used [30,31]. RECIST criteria divided patients into categories (**Table 4**).

Table 4. RECIST categories

Responders:
• Complete responders (CR) when no evidence of residual tumor • Partial responders (PR) when reduction in size of the tumor is more than 30%
Non- responders:
• Stable disease (SD): when tumor size reduction is inferior to 30% • Progressive disease (PD).

MRI examination and image analysis

Before starting the MRI examination, a questionnaire was submitted to each patient to rule out any contraindications (e.g., the presence of cardiac implantable electronic device such as pacemakers or implantable cardioverter defibrillators, implantable neurostimulation systems, cochlear implants, drug infusion pumps and metallic

fragments). Breast MRI was necessarily performed with the administration of a gadolinium-containing contrast agent. Even if gadolinium is a relatively safe contrast agent, we carefully excluded BC patients on dialysis or with a history of renal disease or of allergic or anaphylactic reaction to gadolinium or with high risk factors for nephrogenic systemic fibrosis, with eGFR below 30mL/min/1.73 m^2. Since the contrast enhancement of breast tissue in reproductive age women is dependent on the phase of the menstrual cycle, MRI examinations were performed between the 5^{th} and 12^{th} day after the start of the menstrual cycle. We also excluded the presence of pregnant women, because during pregnancy the administration of contrast agent is predicated on a risk-benefits assessment [35]. Before positioning the patient on the MR table, an intravenous catheter has been placed to administer the contrast agent with a power injector. A dedicated bilateral breast coil was used and each patient was placed in the prone position with both breasts hanging in the coil loops. To avoid motion artifacts, the breasts were no compressed and patient was placed in the most comfortable position. As recommended [26], we performed breast MRI on a high field scanner (1.5- Tesla Magnetom Avanto, Siemens Healthcare) to obtain an optimal spatial resolution and to increase diagnostic detection. A standard MRI protocol was used for each patient, starting with axial turbo inversion recovery magnitude (TIRM) sequences. Indeed, TIRM sequences are useful to identify water-containing findings, such as cysts and myxoid fibroadenomas. Subsequently, axial 3D fast low-angle shot (FLASH) T1- weighted images sequences were performed. FLASH T1-weighted are “dynamic” sequences because they are first performed

before contrast administration and are then repeated multiple timed after contrast administration (0.1 mmol of GD-DTPA/kg of body weight at a rate of 2 mL/s, followed by a 20 mL saline flush). With the dynamic sequences, the radiologist can evaluate the kinetic of the lesion before and after contrast injection, knowing that the contrast between BC and the adjacent tissue is optimal within the first 2 minutes after the injection. Late post-contrast sequences are useful to evaluate whether a lesion continues to enhance showing a "plateau" or if the lesion shows early wash-out of the contrast material [26]. Postprocessing, including subtraction from the pre- and post-contrast series and maximum intensity projection, was performed (**Table 5**).

Table 5. MRI protocol parameters

Sequences	***Fat Saturation***	***TR (ms)***	***TE (ms)***	***FA (°)***	***FOV (mm)***	***Phase FOV***	***Slice thickness (mm)***	***Slice gap (mm)***	***Respiratory state***
TIRM	No	4500	97	150	350	100	384x512	3	Free
Flash 3D T1W	No	11	4.76	25	450	68.8	269x384	1.5	Free

Each breast lesion was finally interpreted and described following the ACR breast imaging reporting and data system (BI-RADS) for breast MRI [36]. In addition, according to the RECIST criteria, evaluating the tumor-response-to-therapies, we considered a complete response when no residual contrast enhancement was found at post- treatment MRI (**Figure 6**). When a residual enhanced lesion was found, a comparison between three dimensional measurements pre- and post-NAC was done.

Figure 6. a) 35-year-old woman with invasive ductal breast carcinoma in the lower outer quadrant of the right breast, who performed breast MRI before starting NAC. b)

after-NAC a complete radiological response was found, confirmed on surgical and histological examination.

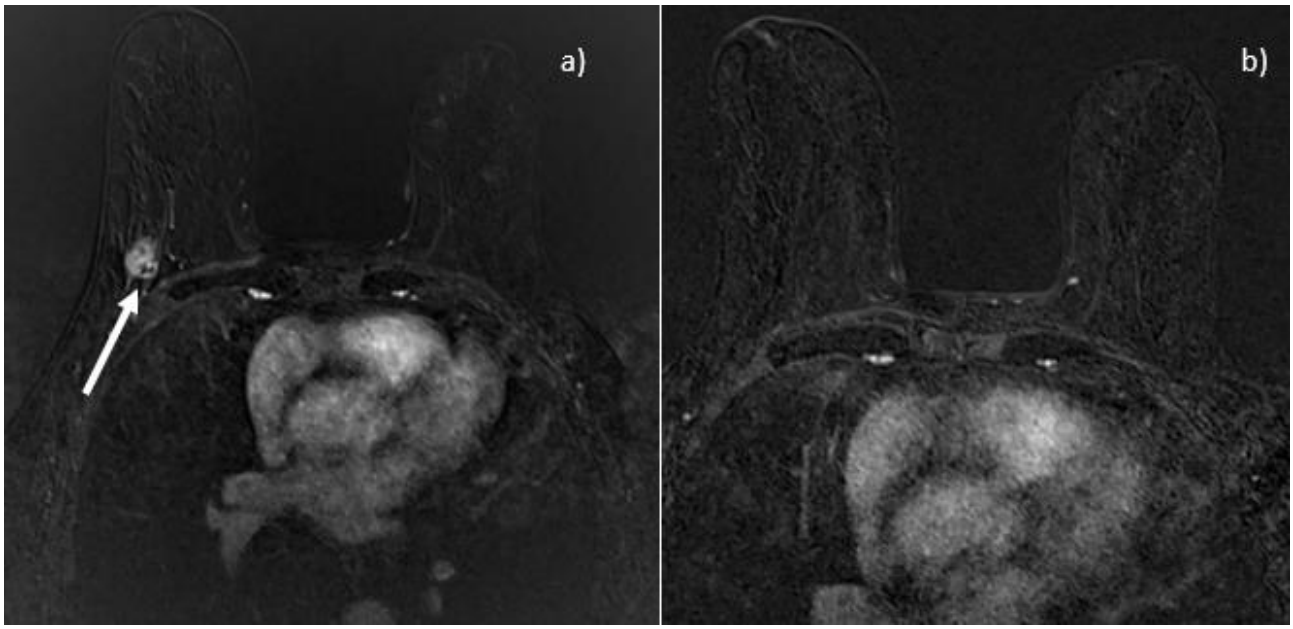

Retrospectively and blindly, two radiologists performed image analysis applying our method, as described before (**Figure 7**). The first radiologist had more than 12 years of experience in musculoskeletal and breast radiology, while the second more than 5 years.

Figure 7. An example of pectoralis muscle area (orange area) contouring on axial 3D Fast Low-Angle Shot (FLASH) T1-weighted images.

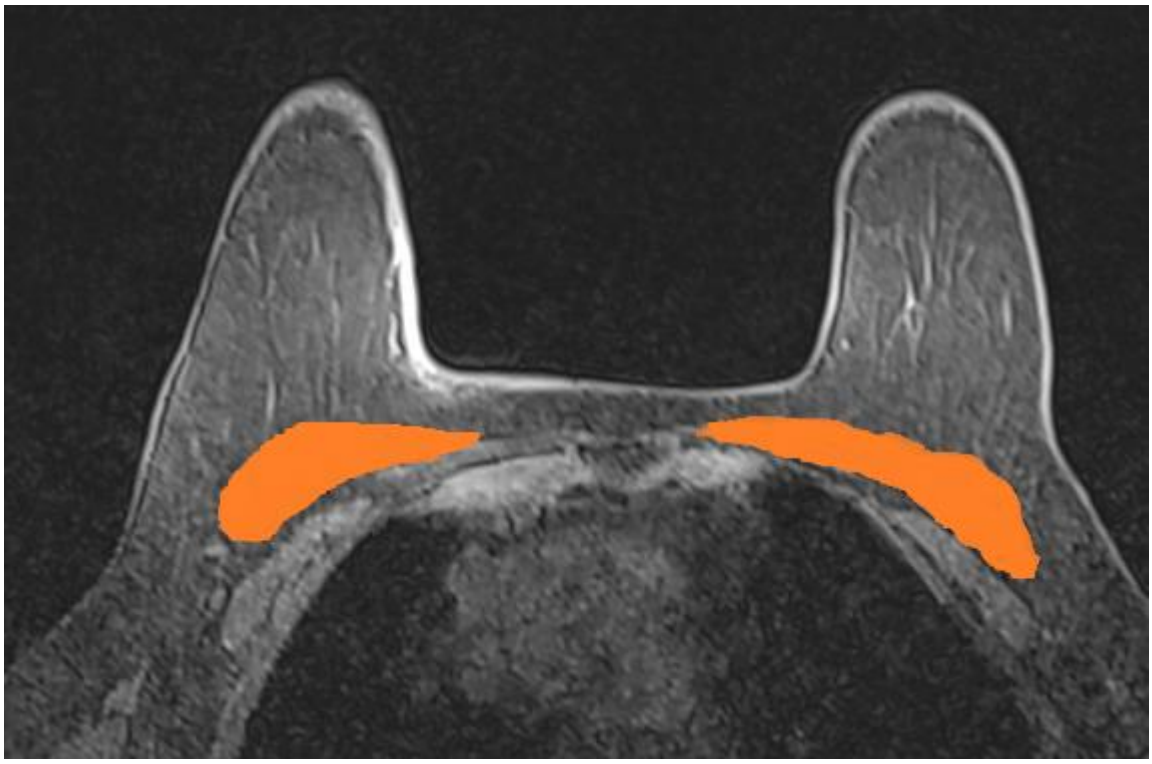

PMA, calculated in square centimeters, was the result of the average of the values obtained bilaterally. To evaluate the reproducibility of the method, we calculated the intra- and inter-reader agreement. To obtain these data, image analysis, as described above, was performed twice, 3 weeks apart. A database was finally created by a third radiologist, who didn't perform the image analysis.

Statistical analysis

Statistical analysis, performed with SPSS version 12.0.1 (SPSS, Inc.), was based on the non-parametric Wilcoxon Mann- Whitney U test, used to compare differences in median values and percentage of PMA calculated on consecutive MRI exams, before and after NAC. The difference between PMA before-NAC and after-NAC was

indicated with ΔPMA. To correlate muscle mass loss with age, time between MRI examinations, ER and PR status, HER-2, Ki-67 expression, lymph node status, RECIST criteria, and different regimes of NAC, a multivariate regression analysis was performed. Cohen's kappa test was finally used to assess the reproducibility of the method, calculating the inter- and intra-reader agreement. We interpreted reliability coefficients as follows: poor, if k value is less than 0.21, fair if k value is between 0.21 and 0.4, moderate if k value results between 0.41 and 0.6, good if k value is between 0.61 and 0.8 and almost perfect is k value results between 0.81 and 1 [37,38]. We considered a p value of .05 as statistically significant.

Results

We selected a total of 65 BC young women of reproductive age (≤45 years), who could have participated in the present study. According to the inclusion criteria, 14 (21.5%) patients were excluded; in particular, 12 patients was ruled out because pre-NAC MRI examination were not available. One patient was excluded for the presence of aesthetic breast implants. Another woman was finally excluded because she had a carcinosarcoma tumor, confirmed by the histopathological analysis. Therefore, a total of 51 young women with invasive ductal carcinoma were finally included. The clinical-pathological data of these selected patients are summarized in **Table 6**.

Table 6. Clinical-pathological data of included patients

Characteristics	**N=51 (%)**
Age (y.o. mean±SD)	37±4.96
BC subtype	
luminal	9/51 (17.7%)
HER2-enriched	22/51 (43.1%)
triple negative (TN)	20/51 (39.2%)
Estrogen receptor	
Positive	28/51 (54.9%)
Negative	23/51 (45.1%)
Progesterone receptor	
Positive	23/51 (45.1%)
Negative	28/51 (54.9%)
Ki-67	
Positive	40/51 (78.4%)
Negative	11/51 (21.6%)
Lymph node status	
Positive	20/51 (39.2%)
Negative	31/51 (60.8%)
Regimes of NAC	
EC followed by Paclitaxel	22/51 (43,1%)
EC followed by Carboplatin and Paclitaxel	8/51 (15.7%)
EC followed by Paclitaxel and Trastuzumab	20/51 (39.2%)
Paclitaxel and Carboplatin	1/51 (2%)
Clinical and radiological response to NAC	
Complete response (CR)	24/51 (47%)
Partial response (PR)	27/51 (53%)
Stable disease (SD)	0
Progressive Disease (PD)	0
PMA (mean ±SD)	
Pre-NAC	9,6±2,6 cm^2
Post-NAC	8,7±2,2 cm^2

The mean age of the patients (± standard deviation) was 37±4.96 years. We found a total of 9 (17.7%) luminal BC subtype, 22 (43.1%) HER2-positive BC and 20 (39.2%) triple negative (TN) disease. A total of 20 (39.2%) patients presented with positive axillary lymph nodes status. Regarding NAC regimes, 22 (43.1%) women were treated with EC followed by Paclitaxel, 8 (15.7%) patients with EC followed by Carboplatin and Paclitaxel, 20 (39.2%) women with EC followed by Paclitaxel and Trastuzumab, while 1 (2%) patient underwent Paclitaxel and Carboplatin. Evaluating

the RECIST criteria, all patients responded to therapy; in particular, a total of 24 (47%) patients were classified as complete responders while 27 (53%) women obtained a partial response. Approximately 158±25.5 days have passed between the two MRI exams (pre- and post- NAC). We found that before-NAC PMA mean value was larger than after-NAC PMA mean value (9.6±2.6 cm^2 vs. 8.7±2.2 cm^2, $p<0.001$, delta value 1.41 ±1.3) (**Figure 8**).

Figure 8. Pre- and post- NAC PMA. PMA assessed pre-NAC (blue line) is larger than post-NAC PMA (red line).

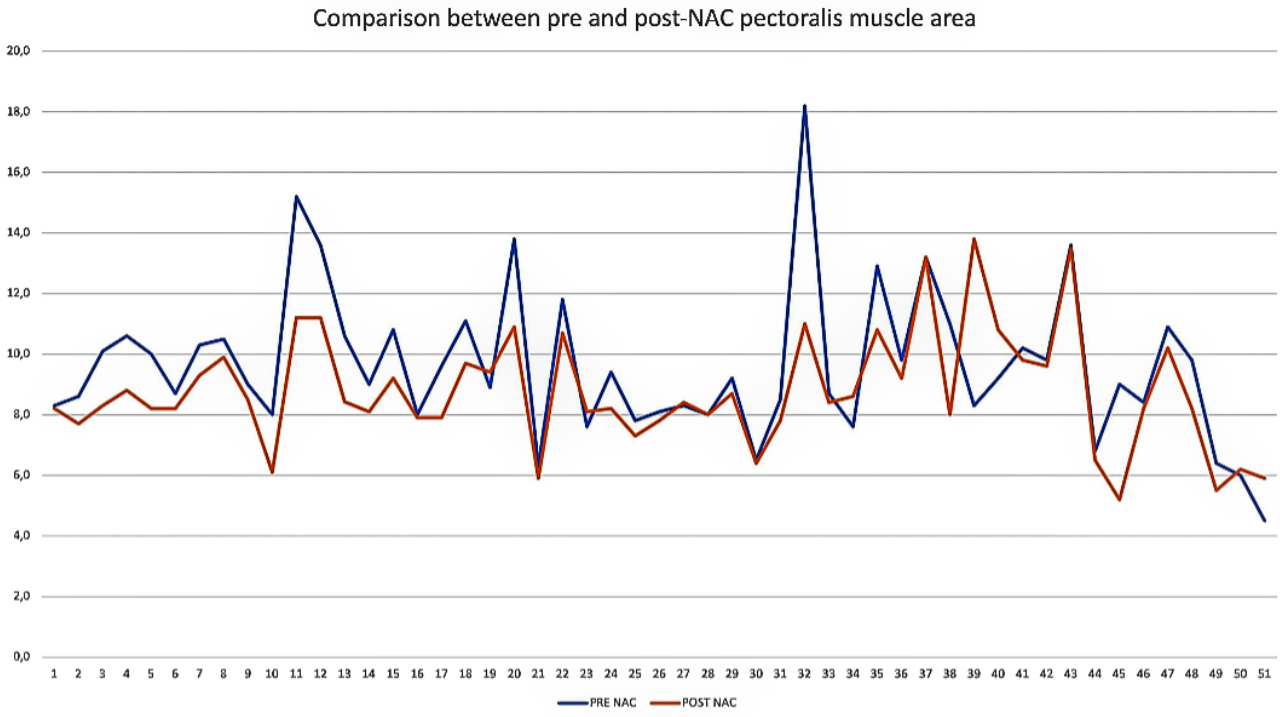

We did not find any significant differences between complete and partial responders in terms of PMA values.

Multivariate regression analysis on ΔPMA

The multivariate regression analysis did not demonstrate statistically significant correlation between PMA variations (ΔPMA) and clinical-pathological characteristics (age of the women, time between MRI exams, ER and PR receptor status, HER-2 status, Ki-67 expression, lymph node involvement, RECIST criteria). No significant correlations were found between ΔPMA and different regimes of NAC.

Inter-reader and intra-reader agreement in PMA assessment

According to Cohen's kappa test, we considered inter- and intra-reader agreement value good (k value between 0.65 and 0.78). Indeed, the inter-reader agreement was k=0.75 (p value <0.05) and the intra-reader agreement of radiologist 1 and radiologist 2 were respectively 0.68 and 0.72.

Discussion

The purpose of this part of research was to evaluate if the PMA, assessed on consecutive standard MRI exams, varies during NAC regimes in young BC patients of reproductive age with IDC. The PMA variation reflects the loss of skeletal muscle mass. In addition, the study aims to correlate sarcopenia with clinical-pathological features, different regimes of NAC and radiological response to therapy. According

to previous studies, body composition changes are considered predictors of BC patient outcome [39,40]. Prado et al. demonstrated that sarcopenia in BC patients who underwent capecitabine treatment was associated with negative prognosis and increased toxicity [18]. Indeed, the loss of skeletal muscle mass results in lower volume drug distribution and in higher drug concentration with consequent difficulty in drug excretion. Amitani et al. showed that muscle mass loss during NAC correlated with worse prognosis, representing an independent predictor of disease-free survival in BC women [41]. In this study, Amitani et al. demonstrated that the 27.4% of all included patients lost more than 3% of muscle mass during NAC treatment with anthracycline and taxane [41]. Indeed, cancer therapy can directly influence body composition activating an important inflammatory response through the activation of cytokines and the up regulation of proteasomes [16]. Among the cytokines activated, TNF-alpha increases protein catabolism with consequent muscle dysfunction and weakness. During chemotherapy, mitochondrial damage leads to cytochrome C reduction and peroxisome proliferation resulting in oxidative stress [16]. These data are consistent with our results, showing a loss of muscle mass during NAC. Indeed, using the non-parametric Wilcoxon Mann-Whitney U test, we found significant differences between pre-NAC PMA and post-NAC PMA, with a delta value of delta value 1.41 ±1.3 ($p<0.001$). Even if, assessing sarcopenia, psoas muscle area calculated on axial body CT is considered the gold standard, previous studies demonstrated a good correlation between psoas muscle mass on CT and muscle mass area measured on MRI [22]. In particular, a good correlation was found between

psoas muscle area assessed on axial body CT and pectoralis muscle area evaluated on breast MRI [22]. Therefore, both imaging modalities (body CT and breast MRI) could be used to assess body composition in BC patients, especially when body CT is not available. Indeed, according to international guidelines, body CT is not used in loco-regional BC diagnosis, especially in early BC, where distant metastases are not frequent [23]. During locoregional BC staging, MRI is strongly recommended especially in the preoperative setting, because it allows to identify multifocal or multicentric or contralateral BC [26]. In addition, according to the American Cancer Society (ACS) and National Comprehensive Cancer Network (NCCN) guidelines, annual breast MRI screening is suggested in young women carrying a BRCA mutation and in familial BC risk young patients [42-45]. MRI in young premenopausal women plays an important role since these patients usually present dense breasts, difficult to study with MX [26]. Moreover, MRI is considered the most accurate imaging modality to evaluate tumor response to NAC [26]. PMA can be evaluated on standard breast MRI examination, without additional sequences, modified protocols or diagnostic delays. Furthermore, PMA assessment on breast MRI is an easily reproducible method between different radiologists, as demonstrated by the good inter- and intra-reader agreement (k value between 0.65 and 0.78). Even if a power analysis was conducted, the multivariate regression analysis did not report any significant relationships between ΔPMA and clinical-pathological features (age, time between MRI examinations, ER and PR status, HER-2 status, Ki-67 expression, lymph node involvement, RECIST criteria, and different regimes of NAC). This

result can be partially justified by the low number of selected patients. Even if BC represents the most common tumor type in young women [32] and even if our University Hospital represents the local reference center for BC, the number of included BC young patients was limited. Indeed, a significant number of patients (n=12) was excluded because pre-NAC MRI examination was not available. Pre-NAC MRI is often performed in peripheral centers, which subsequently refer the patient to our center, where there is a dedicated multidisciplinary team. Indeed, a multidisciplinary team is needed especially for premenopausal women to guarantee optimal care, also offering fertility preservation strategies.

Some limitations of this study need to be known. As already mentioned, although conducted within a prospective study, this is a retrospective analysis with a relatively small study-population. Secondly, we did not divide the patients based on the specific NAC protocol, with consequent potential errors due to the different pharmacokinetic effects on body composition. In addition, for practical reason, we did not evaluate muscle quality and muscle density, analyzing only body composition changes in terms of muscle area depletion. Lastly, cut-off value for sarcopenia, assessed on MRI, have not yet been identified, as was done for sarcopenia assessed on body CT.

To validate our results, further studies are needed, especially to correlate PMA changes with prognostic outcomes. This preliminary study demonstrated the potential application of PMA assessment in young patients with IDC breast cancer undergoing NAC. In addition, PMA can be easily evaluated also during long-term follow-up with breast MRI. PMA assessment on routine breast MRI could help the early diagnosis of

sarcopenia and it could represent a tool for selecting patients worthy of pharmaceutical or other interventions (including physical activity).

In conclusion, this study showed body composition changes in terms of loss of skeletal muscle mass in young premenopausal patients with invasive ductal breast cancer undergoing NAC regimes, whose radiological response was assessed on consecutive breast MRI examinations. PMA variation on breast MRI could be a potential tool to diagnose early skeletal muscle mass loss during NAC, emphasizing the risk of increased chemotoxicities and improving patient outcome.

Conclusions

The conclusion of the entire research can be summarized as follows. Radiological assessment of muscle mass and quality (sarcopenia) in women of reproductive age (≤45 years) or >45 years could be related to muscle loss following NAC regardless other confounding factors. In addition, a novel method to assess the PMA on breast MRI was developed and clinically employed.

My research on sarcopenia and imaging in BC women led to some scientific publications:

1. Muscle mass estimation on breast magnetic resonance imaging in breast cancer patients: comparison between psoas muscle area on computer tomography and

pectoralis muscle area on MRI. Rossi F, Valdora F, Barabino E, Calabrese M, Tagliafico AS. Eur Radiol. 2019 Feb;29(2):494-500. doi: 10.1007/s00330-018-5663-0. Epub 2018 Aug 7.

2. Evaluation of body Computed Tomography-determined sarcopenia in breast cancer patients and clinical outcomes: A systematic review. Rossi F, Valdora F, Bignotti B, Torri L, Succio G, Tagliafico AS. Cancer Treatment and Research Communications 2019; https://doi.org/10.1016/j.ctarc.2019.100154
3. Muscle mass loss after neoadjuvant chemotherapy in breast cancer: estimation on breast magnetic resonance imaging using pectoralis muscle area. Rossi F, Torri L, Lambertini M, De Giorgis S, Calabrese M, Tagliafico AS. Eur Radiol. 2020 Mar 31. doi: 10.1007/s00330-020-06799-5
4. Ultrasound Biomarkers for Sarcopenia: What Can We Tell So Far? Mirón Mombiela R, Vucetic J, Rossi F, Tagliafico AS. Semin Musculoskelet Radiol. 2020 Apr;24(2):181-193. doi: 10.1055/s-0039-3402745. Epub 2020 May 21.
5. Sarcopenia: how to measure, when and why. AS Tagliafico, B Bignotti, L Torri, F Rossi. Radiol Med. 2022 Mar;127(3):228-237. doi: 10.1007/s11547-022-01450-3. Epub 2022 Jan 18.

Our method has been patented:

Patent: 102019000016049 for sarcopenia assessment on pectoralis muscle

Ministero dello Sviluppo Economico

Ricevuta di presentazione

per

Brevetto per invenzione industriale

Domanda numero: 102019000016049

Data di presentazione: 11/09/2019

References

[1] Rosenberg IH. Sarcopenia: origins and clinical relevance. J Nutr. 1997;127:990S–91S

[2] Iannuzzi-Sucich M, Prestwood KM, Kenny AM. Prevalence of sarcopenia and predictors of skeletal muscle mass in healthy, older men and women. J Gerontol A Biol Sci Med Sci. 2002;57:M772–7

[3] Morley JE, Baumgartner RN, Roubenoff R, et al. Sarcopenia. J Lab Clin Med. 2001;137:231–43

[4] Olde Rikkert MG, Rigaud AS, van Hoeyweghen RJ, et al. Geriatric syndromes: medical misnomer or progress in geriatrics? Neth J Med. 2003;61:83–7

[5] Cawthon PM, Lui LY, Taylor BC et al.. Clinical definitions of sarcopenia and risk of hospitalization in community-dwelling older men: the osteoporotic fractures in men study. J Gerontol A Biol Sci Med Sci 2017; 72: 1383–89

[6] Malmstrom TK, Miller DK, Simonsick EM et al. SARC-F: a symptom score to predict persons with sarcopenia at risk for poor functional outcomes. J Cachexia Sarcopenia Muscle 2016; 7: 28–36

[7] Beaudart C, Biver E, Reginster JY et al. Validation of the SarQoL(R), a specific health-related quality of life questionnaire for Sarcopenia. J Cachexia Sarcopenia Muscle 2017; 8: 238–44

[8] Sayer AA, Syddall H, Martin H et al.. The developmental origins of sarcopenia. J Nutr Health Aging 2008; 12: 427–32

[9] Sayer AA, Syddall HE, Gilbody HJ et al.. Does sarcopenia originate in early life? Findings from the Hertfordshire cohort study. J Gerontol A Biol Sci Med Sci 2004; 59: M930–4

[10] Cruz-Jentoft AJ, Bahat G, Bauer J, Boirie Y, Bruyère O, Cederholm T, Cooper C, Landi F, Rolland Y, Sayer AA, Schneider SM, Sieber CC, Topinkova E, Vandewoude M, Visser M, Zamboni M; Writing Group for the European Working Group on Sarcopenia in Older People 2 (EWGSOP2), and the Extended Group for EWGSOP2. Sarcopenia: revised European consensus on definition and diagnosis. Age Ageing. 2019 Jan 1;48(1):16-31. doi: 10.1093/ageing/afy169. Erratum in: Age Ageing. 2019 Jul 1;48(4):601

[11] Anjanappa M, Corden M, Green A, Roberts D, Hoskin P, McWilliam A, Choudhury A. Sarcopenia in cancer: Risking more than muscle loss. Tech Innov Patient Support Radiat Oncol. 2020 Nov 9;16:50-57. doi: 10.1016/j.tipsro.2020.10.001

[12] Leong DP, Teo KK, Rangarajan S, Lopez-Jaramillo P, Avezum A Jr, Orlandini A, et al.; Prospective Urban Rural Epidemiology (PURE) Study investigators. Prognostic value of grip strength: findings from the Prospective Urban Rural Epidemiology (PURE) study. Lancet 2015;386:266–73. PubMed https://doi.org/10.1016/S0140-6736(14)62000-6

[13] Chuang SY, Chang HY, Lee MS, Chia-Yu Chen R, Pan WH. Skeletal muscle mass and risk of death in an elderly population. Nutr Metab Cardiovasc Dis 2014;24:784–91. PubMed https://doi.org/10.1016/j.numecd.2013.11.010)

[14] Janssen I, Heymsfield SB, Wang ZM, Ross R. Skeletal muscle mass and distribution in 468 men and women aged 18-88 yr. J Appl Physiol (1985) 2000;89:81–8. PubMed https://doi.org/10.1152/jappl.2000.89.1.81

[15] Lexell J, Downham DY. The occurrence of fibre-type grouping in healthy human muscle: a quantitative study of cross-sections of whole vastus lateralis from men between 15 and 83 years. Acta Neuropathol 1991;81:377–81. PubMed https://doi.org/10.1007/BF00293457

[16] Davis MP, Panikkar R. Sarcopenia associated with chemotherapy and targeted agents for cancer therapy. Ann Palliat Med. 2019 Jan;8(1):86-101. doi: 10.21037/apm.2018.08.02

[17] Shachar SS, Williams GR, Muss HB, Nishijima TF. Prognostic value of sarcopenia in adults with solid tumours: A meta-analysis and systematic review. Eur J Cancer. 2016 Apr;57:58-67. doi: 10.1016/j.ejca.2015.12.030. Epub 2016 Feb 13. PMID: 26882087

[18] Prado CM, Baracos VE, McCargar LJ, Reiman T, Mourtzakis M, Tonkin K, Mackey JR, Koski S, Pituskin E, Sawyer MB. Sarcopenia as a determinant of chemotherapy toxicity and time to tumor progression in metastatic breast cancer

patients receiving capecitabine treatment. Clin Cancer Res. 2009 Apr 15;15(8):2920-6

[19] Villaseñor A, Ballard-Barbash R, Baumgartner K, Baumgartner R, Bernstein L, McTiernan A, Neuhouser ML. Prevalence and prognostic effect of sarcopenia in breast cancer survivors: the HEAL Study. J Cancer Surviv. 2012 Dec;6(4):398-406

[20] Tagliafico AS, Bignotti B, Torri L, Rossi F. Sarcopenia: how to measure, when and why. Radiol Med. 2022 Mar;127(3):228-237

[21] Zwart AT, Becker JN, Lamers MJ, Dierckx RAJO, de Bock GH, Halmos GB, van der Hoorn A. Skeletal muscle mass and sarcopenia can be determined with 1.5-T and 3-T neck MRI scans, in the event that no neck CT scan is performed. Eur Radiol. 2021 Jun;31(6):4053-4062

[22] Rossi F, Valdora F, Barabino E, Calabrese M, Tagliafico AS. Muscle mass estimation on breast magnetic resonance imaging in breast cancer patients: comparison between psoas muscle area on computer tomography and pectoralis muscle area on MRI. Eur Radiol. 2019 Feb;29(2):494-500

[23] Ferlay J., Ervik M., Lam F., Colombet M., Mery L., Piñeros M., Znaor A., Soerjomataram I., Bray F. Global Cancer Obser-Vatory: Cancer Today. International Agency for Research on Cancer; Lyon, France: 2020

[24] I numeri del cancro in Italia 2019. AIOM-AIRTUM- Fondazione AIOM. www.aiom.it

[25] Gilbert FJ, Pinker-Domenig K. Diagnosis and Staging of Breast Cancer: When and How to Use Mammography, Tomosynthesis, Ultrasound, Contrast-Enhanced Mammography, and Magnetic Resonance Imaging. 2019 Feb 20. In: Hodler J, Kubik-Huch RA, von Schulthess GK, editors. Diseases of the Chest, Breast, Heart and Vessels 2019-2022: Diagnostic and Interventional Imaging [Internet]. Cham (CH): Springer; 2019. Chapter 13

[26] Mann RM, Balleyguier C, Baltzer PA, Bick U, Colin C, Cornford E, Evans A, Fallenberg E, Forrai G, Fuchsjäger MH, Gilbert FJ, Helbich TH, Heywang-Köbrunner SH, Camps-Herrero J, Kuhl CK, Martincich L, Pediconi F, Panizza P, Pina LJ, Pijnappel RM, Pinker-Domenig K, Skaane P, Sardanelli F; European Society of Breast Imaging (EUSOBI), with language review by Europa Donna–The European Breast Cancer Coalition. Breast MRI: EUSOBI recommendations for women's information. Eur Radiol. 2015 Dec;25(12):3669-78

[27] Rossi F, Torri L, Lambertini M, De Giorgis S, Calabrese M, Tagliafico AS. Muscle mass loss after neoadjuvant chemotherapy in breast cancer: estimation on breast magnetic resonance imaging using pectoralis muscle area. Eur Radiol. 2020 Aug;30(8):4234-4241

[28] Korde LA, Somerfield MR, Carey LA, Crews JR, Denduluri N et al (2021) Neoadjuvant Chemotherapy, Endocrine Therapy, and Targeted Therapy for Breast Cancer: ASCO Guideline. J Clin Oncol 39:1485-1505

[29] Sardanelli F, Boetes C, Borisch B et al (2010) Magnetic resonance imaging of the breast: recommendations from the EUSOMA working group. Eur J Cancer 46:1296–1316

[30] Therasse P, Arbuck SG, Eisenhauer EA et al (2000) New guidelines to evaluate the response to treatment in solid tumors. European Organization for Research and Treatment of Cancer, National Cancer Institute of the United States, National Cancer Institute of Canada. J Natl Cancer Inst 92:205–216

[31] Londero V, Bazzocchi M, Del Frate C et al (2004) Locally advanced breast cancer: comparison of mammography, sonography and MRimaging in evaluation of residual disease in women receiving neoadjuvant chemotherapy. Eur Radiol 14:1371–1379

[32] Lambertini M, Pinto AC, Del Mastro L. (2014) Fertility issues in young breast cancer patients: what women want. J Thorac Dis. 2014; 6:584–588

[33] Johnson RH, Anders CK, Litton JK, Ruddy KJ, Bleyer A. (2018) Breast cancer in adolescents and young adults. Pediatr Blood Cancer 2018;65:e27397. doi: 10.1002/pbc.27397. Epub 2018 Aug 28.

[34] Blondeaux E, Massarotti C, Fontana V, Poggio F, Arecco L et al (2021) The PREgnancy and FERtility (PREFER) Study Investigating the Need for Ovarian Function and/or Fertility Preservation Strategies in Premenopausal Women With Early Breast Cancer. Front Oncol 11:690320

[35] Ghadimi M, Sapra A. Magnetic Resonance Imaging Contraindications. [Updated 2022 May 8]. In: StatPearls [Internet]. Treasure Island (FL): StatPearls Publishing; 2022 Jan

[36] American College of Radiology (2013) BI-RADS(r) — MRI. BI-RADS (r) Atlas. 1 ed. Reston: American College of Radiology

[37] Bland JM, Altman DG (2003) Applying the right statistics: analyses of measurement studies. Ultrasound Obstet Gynecol 22:85-93

[38] Landis JR, Koch GG (1977) The measurement of observer agreement for categorical data. Biometrics 33:159–174

[39] Rossi F, Valdora F, Bignotti B, Torri L, Succio G, Tagliafico AS (2019) Evaluation of body Computed Tomography-determined sarcopenia in breast cancer patients and clinical outcomes: A systematic review. Cancer Treat Res Commun 21:1001547

[40] Seo A, Hwang JM, Lee JM, Jung TD (2019) Changes in Pectoral Muscle Volume During Subacute Period after Radiation Therapy for Breast Cancer: A Retrospective up to 4-year Follow-up Study. Sci Rep 9:7038

[41] Amitani M, Oba T, Kiyosawa N, Morikawa H, Chino T et al (2022) Skeletal muscle loss during neoadjuvant chemotherapy predicts poor prognosis in patients with breast cancer. BMC Cancer 22:327

[42] Saslow D, Boetes C, Burke W, Harms S, Leach MO, Lehman CD et al (2007) American Cancer Society guidelines for breast screening with MRI as an adjunct to mammography. CA Cancer J Clin 57:75-89

[43] Warner E, Messersmith H, Causer P, Eisen A, Shumak R, Plewes D (2008) Systematic review: using magnetic resonance imaging to screen women at high risk for breast cancer. Ann Intern Med 148:671-679

[44] Sardanelli F, Podo F, Santoro F, Manoukian S, Bergonzi S, Trecate G et al (2011) High Breast CancerRisk Italian 1 (HIBCRIT-1) Study (2011) Multicenter surveillance of women at high genetic breast cancer risk using mammography, ultrasonography, and contrast-enhanced magnetic resonance imaging (the high breast cancer risk Italian 1 study): final results. Invest Radiol 46:94-105

[45] Lehman CD, Lee JM, DeMartini WB, Hippe DS, Rendi MH, Kalish G et al (2016) Screening MRI in women with a personal history of breast cancer. J Natl Cancer Inst 7;108(3)